

Design of a low-cost and lightweight 6 DoF bimanual arm for dynamic and contact-rich manipulation

Jaehyung Kim¹, Jiho Kim², Dongryung Lee¹, Yujin Jang², Beomjoon Kim¹

¹Kim Jaechul Graduate School of AI, KAIST
{kimjaehyung, dlee960504, beomjoon.kim}@kaist.ac.kr

²Mechanical System & Design Engineering, Seoultech
{wlgh3242, uzzz}@seoultech.ac.kr

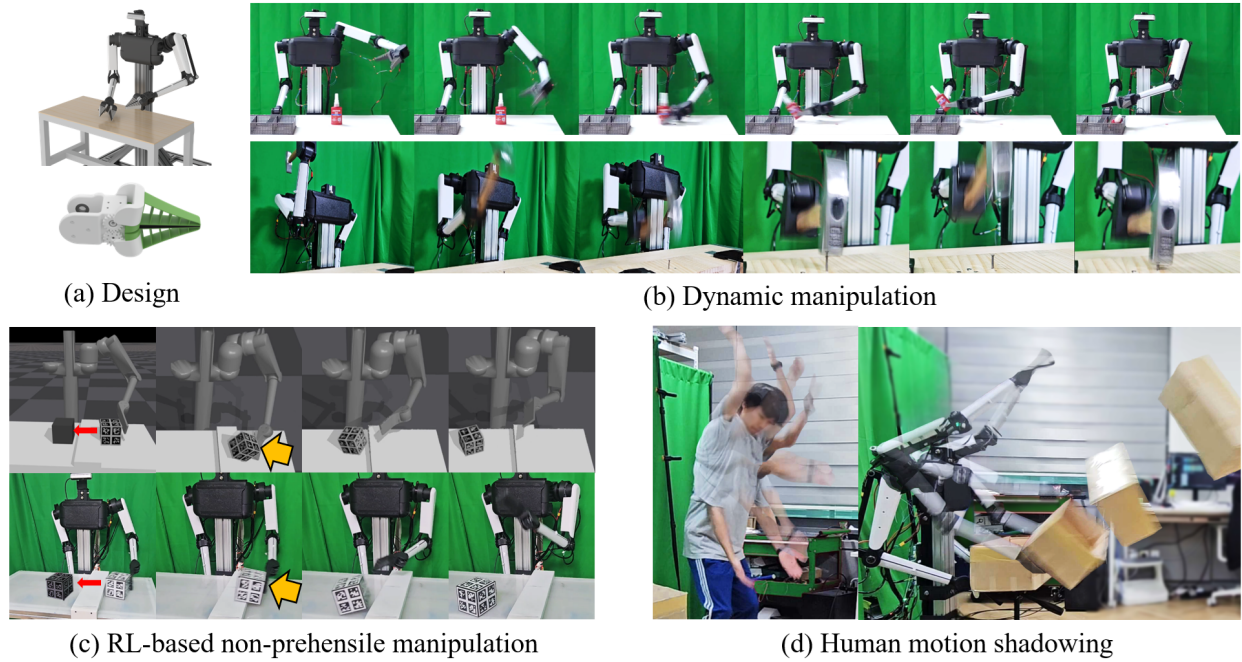


Fig. 1: (a) Illustration of the ARMADA design. (b) ARMADA’s lightweight 6-DoF bimanual arms enable dynamic manipulations such as object snatching and hammering. (c) The platform supports sim-to-real transfer of dynamic motions using reinforcement learning policies. (d) ARMADA also demonstrates the ability to shadow dynamic human movements.

Abstract—Dynamic and contact-rich object manipulation, such as striking, snatching, or hammering, remains challenging for robotic systems due to hardware limitations. Most existing robots are constrained by high-inertia design, limited compliance, and reliance on expensive torque sensors. To address this, we introduce ARMADA (Affordable Robot for Manipulation and Dynamic Actions), a 6 degrees-of-freedom bimanual robot designed for dynamic manipulation research. ARMADA combines low-inertia, back-drivable actuators with a lightweight design, using readily available components and 3D-printed links for ease of assembly in research labs. The entire system, including both arms, is built for just \$6,100. Each arm achieves speeds up to 6.16m/s, almost twice that of most collaborative robots, with a comparable payload of 2.5kg. We demonstrate ARMADA can perform dynamic manipulation like snatching, hammering,

and bimanual throwing in real-world environments. We also showcase its effectiveness in reinforcement learning (RL) by training a non-prehensile manipulation policy in simulation and transferring it zero-shot to the real world, as well as human motion shadowing for dynamic bimanual object throwing. ARMADA is fully open-sourced with detailed assembly instructions, CAD models, URDFs, simulation, and learning codes. We highly recommend viewing the supplementary video at <https://sites.google.com/view/im2-humanoid-arm>.

I. INTRODUCTION

Humans use a rich set of action repertoire to manipulate objects: we not only pick-and-place objects but also toss laundry, slide a box, snatch a pen, hammer a nail, otherwise

leverage momentum and forces to manipulate diverse objects efficiently and effectively. In contrast, most manipulators today are limited to picking, where a robot simply grasps an object to resist the frictional force. While kinematic pick-and-place is sufficient for static, controlled tasks, dynamic manipulation is necessary for building an effective general-purpose robot.

One critical reason for the lack of dynamic manipulation capability is hardware. Traditional industrial robots are strong, precise, and consistent, but their heavy and high inertia structures make them unsuitable for dynamic manipulation in human environments. Modern collaborative robots, such as the Franka Panda [21], are designed to work alongside humans by using a lighter and smaller design. However, they still have high inertia and are constrained by velocity and torque limits to ensure safety, rendering them inadequate for dynamic manipulation that requires high speed and acceleration. Furthermore, they use high gear ratio actuators which effectively “lock” joints, making them difficult to absorb high impact forces at contacts. Such actuators also require expensive torque sensors, as current-to-torque relationship is difficult to model due to the backlash and friction caused by multi-stage gears.

Our objective is to build and open-source a 6 degrees-of-freedom (DoF) bimanual robot that can be easily and cheaply assembled at a lab to democratize dynamic manipulation research, such as examples shown in Figure 1. To achieve this, our design must meet the following criteria:

- **Dynamic:** the robot should be able to move at high speed with acceleration to perform dynamic manipulation.
- **Low-cost:** the design should use inexpensive materials, sensors, and actuators while having high payload, precision, and torque necessary for versatile manipulation.
- **Safe:** the robot should have a low inertia to ensure safety even at the maximum speed.
- **Ease of assembly:** the robot should be built with off-the-shelf materials.

One potential way to achieve these is through tendon drive systems [54, 46, 20]. These systems transmit torques to joints located far from motors, allowing actuators to be placed at the arm’s base. This design significantly reduces inertia and enhances the robot’s agility. Furthermore, tendons are highly back-drivable, making them well-suited for rapid and dynamic movements.

However, tendon-driven robots have several problems. First, they are difficult to assemble and maintain at a research lab. Assembling a tendon-wiring mechanism involves integrating multiple pulleys connecting tendons to rotors while avoiding interference with electronic connections, an intricate and complex task. Achieving the desired levels of stiffness and friction adds another layer of complexity, as it requires precise adjustment of tendon tension through a tensioner. Moreover, tendon-driven systems are susceptible to wear and tear, particularly during high-impact tasks such as hammering. In such scenarios, tendons may loosen upon impact, necessitating frequent adjustments and repairs to maintain performance.

We instead take inspiration from the recent success of quadrupeds in designing our bimanual robot. Recent

quadrupeds demonstrate dynamic and explosive movements, such as jumping and parkour [27, 12], while reliably withstanding high-impact, high-frequency contact forces. What enables this is the use of quasi-direct drive (QDD) actuators, which have significantly lower gear ratios compared to those typically used in collaborative robots (eg., 1:10 vs. 1:100). These low-gear ratio actuators make the system highly back-drivable, allowing joints to absorb impact forces through natural compliance. Additionally, the reduced backlash and friction in these actuators simplify modeling the current-to-torque relationship, eliminating the need for expensive torque sensors.

To minimize inertia, we would ideally move all the actuators to the body, as done in quadrupeds. However, the key difference between a quadruped leg and a bimanual arm is the number of joints. While a quadruped leg typically has 3 DoF, with only the knee joint located away from the body, a robot arm requires at least 6 DoF to achieve full spatial manipulation. To address this, we mount heavier and stronger actuators on the main body to control the shoulder joints, and use smaller, lighter actuators for the elbow and wrist joints. This design results in a lighter moving mass, albeit at the cost of reduced strength in the elbow and wrist.

Figure 1a top showcases our robot, ARMADA (Affordable Robot for Manipulation and Dynamic Actions), built with these design principles. Each arm weighs 1.09 kg (excluding body-mounted parts and gripper) and is constructed using off-the-shelf motors and 3D-printed links. The entire system costs \$6,100 to build. To eliminate the need for a torque sensor at each joint, we manually measured and calibrated the current-to-torque relationship¹. To improve impact resistance and ease of assembly, we use a linkage-based transmission mechanism that does not require tensioners. The robot’s links are 3D-printed using polylactic acid (PLA), except for the elbow joint, which is made from aluminum to reduce deformation under high loads.

We also develop a simple, compact jaw gripper compatible with the arm shown in Figure 1a bottom. By using the thermoplastic polyurethane (TPU) based finger without linkage structure, this design simplifies construction and maintenance while providing sufficient robustness for dynamic tasks. The gripper design, like the rest of ARMADA, is fully open-sourced.

In our experiments, we show ARMADA could perform several dynamic motions, such as object snatching and hammering. We also demonstrate we can train a contact-rich non-prehensile manipulation policy entirely in simulation using reinforcement learning (RL), and zero-shot transfer to the real world. Lastly, we show ARMADA can be used for human motion retargeting on the dynamic bimanual object throwing task. Examples from these tasks are highlighted in Figure 1. We completely open-source our code and design.

¹vendor’s data was inaccurate

II. RELATED WORK

A. Existing manipulators in the context of dynamic manipulation

Classical industrial robots, such as Unimate [15], PUMA [7], and SCARA [42], were among the earliest programmable robots designed for efficient manipulation in factory settings. They perform quasi-static tasks such as assembly, die casting, and welding, with exceptional precision and consistency. However, their high inertia structures render them unsuitable for dynamic tasks. Optimized for fixed and controlled factory environments, these robots lack the agility required for frequent contact or rapid movements required for dynamic manipulation.

Collaborative robots (cobots), such as the Franka Emika [21] and KUKA LBR series [25, 26, 3], are designed to operate in humans environments. One significant limitation of cobots is their reliance on high-gear-ratio actuators, which introduce uncertainties in joint dynamics due to gearbox backlash and friction. Because of this, to achieve precise torque control, cobots often incorporate torque sensors; however, these sensors are susceptible to damage from impacts, and are expensive [62]. Furthermore, while cobots are smaller in size, they still have the same design structure as industrial robots, with heavy actuators (around 2 kg) placed at each joint, which results in a high-inertia arm.

The dominant approach for designing robots for dynamic manipulation is to use tendon transmissions to achieve low inertia and absorb impact forces. Barrett WAM [48] uses a cable-and-cylinder drive system to mount four motors for the shoulder and elbow joints on the robot's body, resulting in a low-inertia 4 DoF arm capable of tasks such as batting and throwing. Similarly, Quigley et al. [46] incorporate series-elastic actuators at the shoulder and elbow joints with tendon-based transmission to achieve low inertia. LIMS [35, 54] attach all seven actuators to the main body and control joints via tendons. Coupled with lightweight link designs, it can perform dynamic tasks such as swinging folding fans. PAMY2 [20] combines tendon-driven transmissions with pneumatic artificial muscles for passive compliance in a 4 DoF arm, demonstrating dynamic capabilities such as table tennis smashing. Nishii et al. [44] uses a combination of timing belts and tendons. It uses a timing belt to attach four motors near the body, and a tendon-based quaternion joint mechanism for the 2 DoF wrist, achieving 6 DoF maneuverability with reduced moving mass.

Tendon-based systems generally achieve low inertia and gear ratio, and enable quick, explosive, and dynamic movements. However, maintaining tendons requires precise tensioning to achieve proper stiffness and friction, and it is very difficult to assemble them. These systems also face wear and tear during high-impact tasks, requiring frequent repairs. We summarize the comparison among ARMADA and existing manipulators in Table I.

B. Dynamic movements in quadrupeds

The state-of-the-art quadruped hardware, combined reinforcement learning, has shown impressive dynamic motions such as jumping and parkour recently [63, 12, 14]. Representative quadruped hardware includes, but is not limited to, Unitree Go1, MIT Cheetah [8], KAIST Hound [53], and Raibo [14]. One common factor in all these hardware platforms is the use of quasi-direct-drive (QDD) actuators [56]. Since QDD actuators have fewer gear stages, they have much less backlash and friction compared to high-gear ratio actuators (See Figure 2). Further, their back-drivability makes them naturally compliant, enabling them to absorb high-impact forces, and allows us to model the current-to-torque relationship much easier. We take inspiration from these successes, and adopt QDD in our arms.

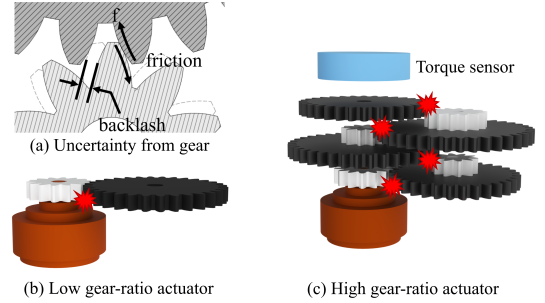


Fig. 2: Comparison of gearboxes in low-gear ratio actuators (b) vs. high-gear ratio actuators (c). All gear mechanisms introduce backlash and friction (a) which are difficult to model. Because low gear ratios use fewer gears, it is easier to model.

Another essential design principle in recent quadrupeds is the use of low-inertia legs, typically achieved by mounting actuators on the body and connecting them to the legs via transmission systems such as timing belts or linkages. This approach minimizes the moving mass, enabling the legs to move rapidly while using less torque. In our arm, we also employ linkages as our transmission system to control the elbow joint since it is easier to assemble, and locate as many actuators as possible to the robot's body. However, unlike quadrupeds, our arm features six degrees of freedom (6 DoF) and requires additional degrees of freedom at the wrist. To address this and maintain low inertia, we use lighter, weaker actuators at the wrist since high torque is generally not required in these parts region.

C. Hardware solutions for high-impact manipulation

For dynamic and contact-rich tasks, robustness against impact forces is essential. Several works have proposed hardware solutions to address this in high-impact scenarios such as hammering. Izumi et al. [30] utilize a flexible link to minimize impulsive forces, and Garabini et al. [17] use actuators with torsional elastic springs to absorb impact while achieving high speeds. Both approaches model the system to control and demonstrate the hammering task but require accounting for damping forces and vibrations from elastic components, making them difficult to simulate. Instead of mitigating impact

TABLE I: Comparison of manipulators

	ARMADA (Ours)	Franka Panda [21]	KUKA iiwa 7 R800	Quigley et al. [46]	LIMS [36]	Nishii et al. [44]	PAMY2 [20]	BLUE [18]
DoF (one arm)	6	7	7	7	7	6	4	7
Inertia (kg·m ²)	0.234	large	large	0.083	0.599	?	?	0.75
Moving mass ¹ (kg)	1.09	18	22.3	2	2.24	0.176	1.3	8.7
End-effector speed (m/s)	6.16	1.7	3.2	1.5	5.35	?	12	2.1
Total cost (\$, one arm)	3,040	expensive	expensive	4,135	?	?	14,540	<5,000
Open-source	O	X	X	O	X	X	O	O
Payload (kg)	2.5	3	7	2	3	3	?	2

“?” denotes information not provided in the paper.

¹ moving mass is defined as the arm’s mass, excluding body-mounted components and the gripper.

forces with elastic materials, ARMADA adopts QDD actuators to make the system inherently compliant which simplifies modeling and simulation.

Other designs [29, 47] focus on adding links or control modes to manage impact forces for hammering. Imran et al. [29] introduce serial linkage chains around the robot links to distribute impact forces, while Romanyuk et al. [47] employ MRR actuators [40] with multiple working modes. By switching to a passive mode during impacts, these actuators allow free rotation to absorb impulsive forces. Although these design choices effectively absorb impacts, additional links or control modes complicate the robot’s design, making them harder to assemble and control. Instead of increasing complexity, ARMADA uses a simpler design with just a four-bar linkage and QDD actuators, ensuring ease of assembly and control while maintaining robustness to impacts.

D. Dynamic manipulation with existing manipulators

There have been several attempts to generate dynamic manipulation motions using existing arms, although they have been limited to one specific category of motion such as throwing, catching, or batting. For throwing, Senoo et al. [51] models contact at the robot fingertip to throw with the WAM robot (4 DoF). Bombile and Billard [9] formulate modulated dynamical systems of a pair of KUKA LBR to toss a box with dual manipulators. Recently, some works using learning to account for the physical properties not explicitly considered in the projectile mechanics from perceptual input, using a Tx60 (7 DoF) [28], a single PR2 arm (7 DoF) [19], and UR5 (6 DoF) [59].

For catching, Lampariello et al. [37] model the motion of 7 DoF manipulator (KUKA LBR) as a dynamical system and propose real-time online optimization algorithms to catch an object tracked with a vision-based motion capture system. Kim et al. [34] leverage expert demonstration to guide the same 7 DoF manipulator to catch more diverse objects. Bätz et al. [6] predicts the trajectory of a flying ball and plausible interception points computed offline to catch the ball with Staubli RX90B (6 DoF). These works focus on the light object which induces negligible impulse since the aforementioned manipulators lack compliance to cope with the large impact generated during the catching of heavier objects. Salehian et al. [49] and Yan et al. [57] attempt to mitigate the impact in the non-compliant manipulator (KUKA LBR) by separately planning a decelerating motion after the intercept of the object. However, additional computation is required for such motion,

which often results in failing to plan the motion before the object falls. Unlike these robots, ARMADA is naturally compliant and can avoid such additional computation. Similarly, Kim et al. [33] enables fast catching with a compliant Barret WAM (7 DoF), yet maintenance of the robot is difficult due to its tendon-based mechanism.

For batting, Senoo et al. [50] develop a high-frequency vision system to track a ball and bat it with a Barrett WAM (4 DoF) using handcrafted batting dynamics. Similarly, Jia et al. [31] model 2D impact dynamics with Coloumb friction and energy-based restitution to bat an object to a desired position with the same 4 DoF manipulator. Although these methods enable dynamic batting with light objects like styrofoam or ping pong balls, it is difficult to use them with heavier objects with existing arms, as hitting heavy objects might damage the manipulator. In contrast, ARMADA is naturally compliant, and is easy to maintain.

E. RL-based Manipulation

Recently, reinforcement learning (RL) has been successfully applied to contact-rich manipulation tasks, including in-hand manipulation [11, 5, 4, 22] and non-prehensile manipulation [61, 60, 13, 32], addressing challenges that traditional planning techniques have struggled to solve. These advancements have been made possible through the combination of large-scale simulation and simulation-to-reality transfer techniques, such as domain randomization. However, most of these works rely on cobots, which are less suited for quick and dynamic motions involving frequent impacts limiting them to slow movements. In contrast, we demonstrate that our robot can achieve similar non-prehensile manipulation tasks using RL while exhibiting much more agile and dynamic motions.

F. Human motion shadowing

Thanks to the recent development of computer vision algorithms, several works show that we can collect human demonstrations simply by watching them. H2O [24] and OmniH2O [23] adopts HybrIK [38] as body pose predictors to achieve real-time humanoid teleoperation using a RGB camera. HumanPlus [16] leverages human body [52] and hand [45] pose predictors to extract human joint angles in real time and project them on the humanoid actuators. Similarly, OKAMI [39] adopts body [58] and hand [45] pose predictors to extract human body keypoints and solve differential inverse kinematics [10] to imitate human motion that keeps the relative positions between the hands similar to that of human. Leveraging a single RGB camera with body pose predictor [52]

we showcase that our hardware, ARMADA, also is capable of shadowing human demonstrations in dynamic bimanual throwing.

III. DESIGN OF ARMADA

This section describes our hardware design and implementation details. Our primary goal is to achieve high-speed manipulation with low gear-ratio proprioceptive actuators while maintaining sufficient durability and ease of maintenance.

A. Proprioceptive actuators

1) *Choice of actuators:* We choose two types of off-the-shelf proprioceptive actuators: T-motor AK70-10 for shoulder and elbow and Cubemars RMD X4 V2 for wrist and forearm. Both types have 1:10 gear ratio with integrated drivers. Each arm is powered by two 24V Mean Well LRS-600-24 switch mode power supplies (SMPS). To protect the power supply from the back electromotive force generated by the actuators, SEMI-REX MD110-16 diodes are installed between the power supply and the actuators.

2) *Sensor-free torque estimation for control:* Instead of using expensive torque sensors, we estimate the torque output from the actuators by building a custom current-to-torque function using our custom calibration process. To do this, we fix an actuator to a 3D-printed fixture connected to a standard electronic scale, measure the torques by giving a wide range of current values, and create a linear interpolation mapping between current and torque values. We extrapolate to estimate values beyond the available data range to compute the torque.

B. Actuator placement and transmission

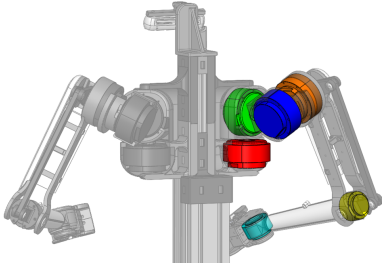


Fig. 3: Positions of the six actuators. Four heavy and strong actuators are attached to the base. Two small actuators to rotate the wrist is attached to the elbow and wrist.

1) *Low inertia actuator placement:* ARMADA arm features 6 DoF: three on the shoulder, one on the elbow, and two on the wrist. We place the shoulder and elbow actuators near the base as illustrated in Figure 3. By positioning the heavy actuators near the shoulder and transmitting the motion via the linkage system, we can effectively reduce the moment of inertia of the arm, achieving faster motion with the same amount of power from the actuators. We attach the two weaker but lightweight actuators directly on the elbow and wrist to keep the design simple.

2) *Parallelogram linkage for one-to-one torque transfer:* One of the body-mounted actuators drives the elbow joints through a four-bar parallelogram linkage, as illustrated in Figure 5a. This linkage transfers torque in 1:1 ratio, preserving the low gear ratio of the actuator and simplifying the model used in simulation and control.

C. Material selection

We primarily build the arm using 3D printing with PLA. This choice of material provides several advantages. First, compared to metals, which are the common choice for existing robot arms, PLA greatly reduces the total mass of the arm. Second, 3D printing is cost-effective and enables rapid part replacement for design iteration and maintenance. One disadvantage of PLA is that it is non-rigid compared to metals. This may harm the durability of the hardware and reduce control accuracy when exposed to high loads. Therefore, for the linkage for the elbow, where high loads are applied, we use aluminum, as shown in Figure 5a. This way, we minimize the complicated and costly machining process while maintaining the rigidity sufficient for manipulation. To validate that our robot attains enough rigidity, we perform finite element method (FEM) analysis. Specifically, we assess the arm's deformation under a 10 N load applied along the x-axis (leftward) and the z-axis (downward).

Figure 4 illustrates the deformation results under z-axis and x-axis loading, respectively. Although this material change involves a trade-off with an increase in moving mass from 0.962 kg to 1.09 kg, it reduces deformation under loading conditions. For z-axis loading, the deformation decreases from 1.69 mm with PLA components to 1.58 mm with the addition of aluminum. Similarly, for x-axis loading, the deformation is reduced from 2.85 mm to 2.24 mm.

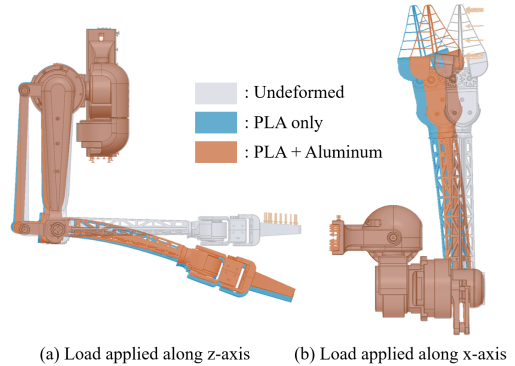
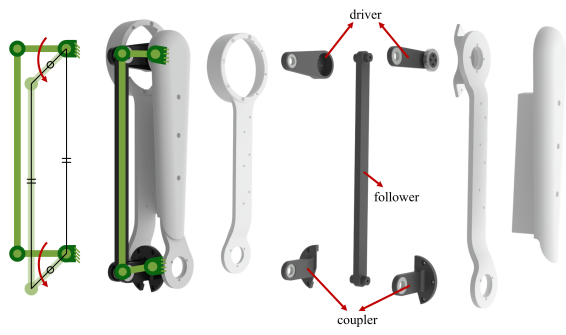


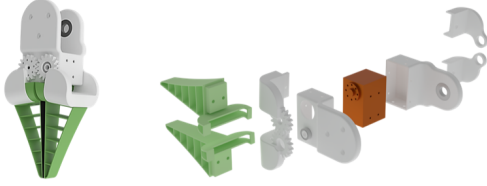
Fig. 4: FEM analysis of deformation under a 10 N load applied along the (a) z-axis and (b) x-axis for configurations with all PLA and partially aluminum components. Deformation reduces from 1.69 mm to 1.58 mm (z-axis) and 2.85 mm to 2.24 mm (x-axis) with aluminum reinforcement. Deformation is exaggerated for clarity and visualization.

D. Custom gripper

We also design a compact jaw gripper driven by a Dynamixel XM430 motor. The gripper utilizes a simple direct-



(a) Arm assembly



(b) Gripper

Fig. 5: (a) Assembly of the upper arm. Black parts are aluminum-machined, and white parts are 3D printed PLA. (b) Assembly of the custom-designed gripper. The brown component is the Dynamixel XM430 motor, the white parts are PLA parts, and the green parts are flexible TPU fingers.

drive 1 DoF gear mechanism, enabling jaw manipulation while maintaining ease of assembly. The gear mechanism is made of PLA, while the gripper pads are printed from flexible TPU to accommodate objects of various shapes. The entire assembly weighs approximately 290 g. Figure 5b illustrates the design of the gripper.

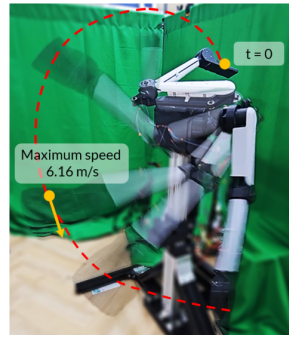
IV. MECHANICAL ANALYSIS

A. End-effector speed

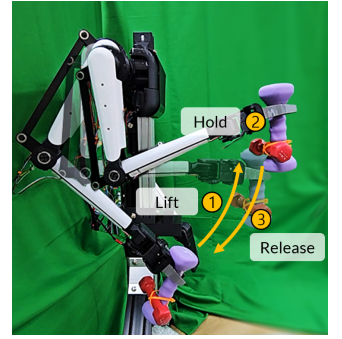
To test whether ARMADA can perform dynamic manipulation, we measure its end-effector maximum speed. To do this, we initialize the robot with its right end-effector positioned at the opposite shoulder with the elbow completely flexed, and then fully extend the elbow downward, as shown in Figure 6a. The joint trajectory is generated by interpolating between the initial and final configurations, and joint position control is used to follow the trajectory. ARMADA achieves an average maximum end-effector speed of 6.16 m/s with a standard deviation of 0.472 m/s across 40 repetitions, without any damage to the arm or power supply.

B. Impact force at the maximum velocity

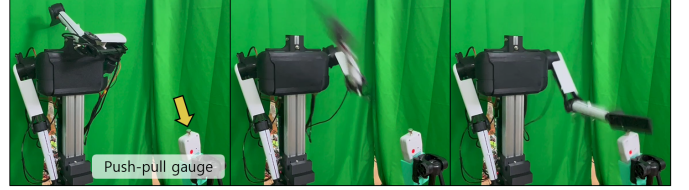
To evaluate the safety of ARMADA, we measure its impact force near maximum velocity using a push-pull gauge, as shown in Figure 6c. Over eight repetitions, ARMADA records an average impact force of 50.5 N, with a maximum of 52.2 N and a standard deviation of 5.55 N. For comparison, a typical human palm strike at a similar speed generates approximately 575 N of impact force, based on an average effective hand mass of 1.39 kg [2] and an impact duration of 13 ms [55],



(a) Speed test



(b) Lifting test



(c) Impact test

Fig. 6: (a) Trajectory of the end-effector speed test. Starting from the initial joint position, ARMADA accelerates toward the terminal position. (b) A sequence of a realistic dumbbell lifting task. The robot grasps, lifts, holds for three seconds, and places down the dumbbell. (c) We use push-pull gauge to measure the maximum impact force near the point of maximum speed.

which is nearly 10 times that of ARMADA. While humans have soft skin and ARMADA does not, this demonstrates ARMADA can operate safely even at its maximum speed.

C. Payload

We evaluate ARMADA's payload using dumbbells, as shown in Figure 6b. The test involves performing bicep curls with the dumbbell. By gradually increasing the weights, we find that ARMADA can hold up to 2.5 kg, compared to 3 kg for existing collaborative robots. The arm and gripper reliably grasp, lift, hold, and release the weight across ten consecutive trials without any damage or failure.

We analyze both mechanical stress and current to evaluate the reliability under the maximum payload. To measure mechanical stress, the robot configuration is set to position 2 in Figure 6b. Each link's stress limit is determined by its tensile strength, which is defined as the material's resistance to breaking under tension. Using FEM analysis in Ansys, as shown in Figure 7a, we find that the maximum stress experienced by the arm while lifting a 2.5 kg payload is 49.8 MPa, which is within the tensile strength of the PLA filament, 61 MPa. This indicates that ARMADA would deform, but not break and can safely operate under its maximum payload without significant risk of structural failure.

Each actuator has a nominal current limit, the maximum current it can handle without overheating. To evaluate whether the robot operates safely within this limit, we measure the input current throughout the entire payload test including

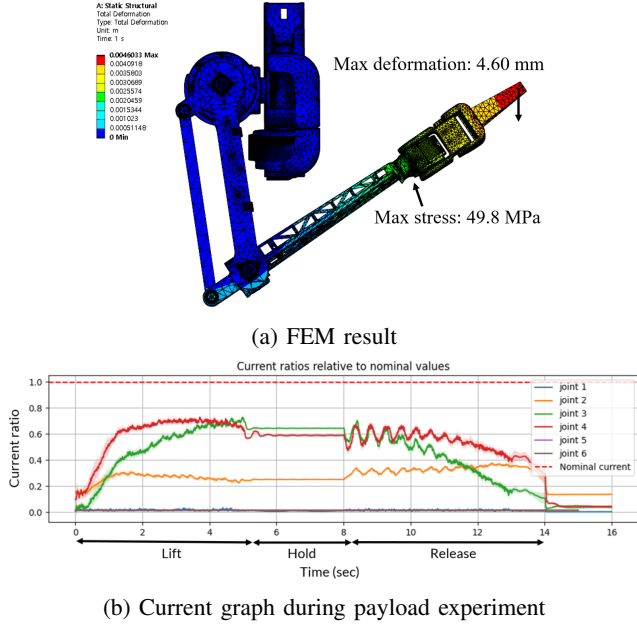


Fig. 7: (a) FEM analysis under a 2.5 kg payload in position 2 in Figure 6b. Maximum deformation occurs at the gripper tip, measuring 4.60 mm, while the maximum stress is observed at the wrist link at 49.8 MPa. Note that the material of the TPU-based gripper is replaced with PLA for FEM analysis, as it is difficult to accurately simulate TPU’s flexibility. (b) The average ratio of actuator current to its nominal value for each actuator and their standard deviations, measured during ten repetitions under a 2.5 kg payload.

lifting, holding, and releasing. Figure 7b shows the current ratios relative to nominal values for each actuator. We can see that all currents are under their nominal values.

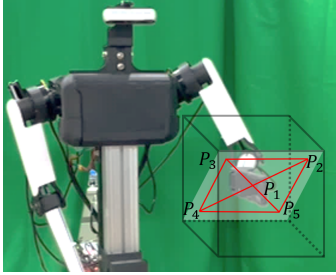


Fig. 8: Repeatability test setup with five end-effector points P_1 to P_5 . The test plane is placed diagonally within the 250 mm cube. P_1 is positioned at the center of the plane, while P_2 , P_3 , P_4 , and P_5 are near the corners, each located one-tenth of the cube’s diagonal length from the center.

D. Repeatability

To evaluate ARMADA’s repeatability, we follow ISO 9283 standard [1] to setup an experiment where the robot has to follow a designated set of points in a 250mm cube within ARMADA’s workspace. Figure 8 shows a test plane placed

diagonally within the cube. Five end-effector points P_1 to P_5 are marked on the plane, with P_1 at the center and P_2 , P_3 , P_4 , and P_5 near the corners, each located one-tenth of the cube’s diagonal length from the center. ARMADA sequentially moves through these five points and repeats the trajectory 30 times with its end-effector facing forward. We use 12 OptiTrack cameras monitor it simultaneously to record the end-effector’s position. For each point, $N = 30$ is the total number of measurements, and $P_i \in \mathbb{R}^3, i = 1, 2, \dots, N$ is the measured position at the i^{th} instance. The ISO 9283 standard states that the mean position of the end-effector $\bar{P} = \frac{1}{N} \sum_{i=1}^N P_i$ is calculated as the average of the measured positions P_i . The repeatability R is computed based on the average (μ) and the standard deviation (σ) of the distances between \bar{P} and P_i .

$$\mu = \frac{1}{N} \sum_{i=1}^N \|P_i - \bar{P}\|, \quad \sigma = \sqrt{\frac{1}{N-1} \sum_{i=1}^N (\|P_i - \bar{P}\|)^2}$$

$$R = \mu + 3\sigma$$

As shown in Table II, ARMADA achieves an average repeatability of 2.63 mm which means it is less consistent compared to the cobots with high gear ratio actuators, whose repeatability is around 0.1mm. This shows the trade-off between compliance and consistency.

TABLE II: ISO 9283 repeatability experiment results

Point	Average distance (mm)	Std dev. (mm)	Repeatability (mm)
P_1	1.048	0.546	2.687
P_2	1.042	0.409	2.269
P_3	0.939	0.689	3.006
P_4	0.751	0.520	2.311
P_5	1.104	0.584	2.857
Average	0.977	0.550	2.626
Franka Panda [21]			0.1
KUKA iiwa 7 R800			0.1
Quigley et al. [46]			*3
LIMS [36]			0.43
Nishii et al. [44]			*2.2
BLUE [18]			*3.7

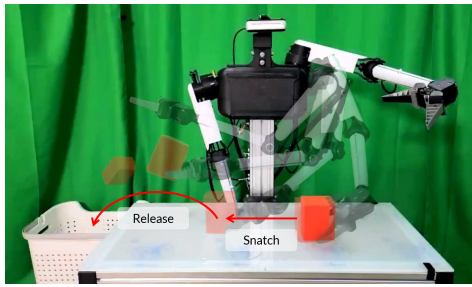
“*” indicates that repeatability is obtained manually, not by ISO 9283.

V. EXPERIMENTS

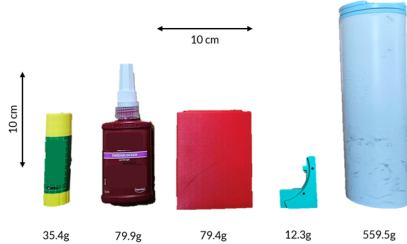
A. Dynamic manipulation

We conduct two experiments, snatching and hammering, to show that ARMADA can perform dynamic manipulation. In these experiments, the target object pose is known in advance, and a pre-defined trajectory is executed with a joint position control to focus on demonstrating raw hardware capability.

1) **Snatching**: Unlike static pick-and-place, snatching involves swift single-arm manipulations, where the robot rapidly approaches, grasps, and releases the target object. The experiment setup is shown in Figure 9a, where the goal is to snatch the object and releases it into a basket beside the table. We test ARMADA with five objects of varying shapes and masses, with ten trials for each object. Detailed information on the sizes and masses of these objects is described in Figure 9b. ARMADA achieves an overall success rate of



(a) Experiment setup



(b) Objects for snatching

Fig. 9: (a) Snatching experiment setup. The object is placed in a fixed pose, and ARMADA rapidly snatches and releases it into the white basket. (b) Various real-world objects used in snatching which have different sizes and masses.

80%, successfully completing all trials and objects except for the heavy tumbler, as shown in Table III. This highlights the strength and limitation of ARMADA, and the difficulty of snatching. While it can snatch light-weight objects, it often drops the heavy tumbler (560 g) after snatching. Such heavy object demands a much more delicate yet firm grasp to counteract momentum and gravity effectively. Please see our supplement videos on snatching for better visualization.

TABLE III: Snatching experiment results

Object	Glue	Threadlocker	Plastic box	Bracket	Tumbler	Total
Success/Trial	10/10	10/10	10/10	10/10	0/10	40/50

2) **Hammering**: This task involves repeatedly striking a nail into a wooden board to evaluate the robot’s capability of creating significant impact force. The experiment setup is shown in Figure 10. We record the number of strikes required to drive the nail 20 mm into the wooden board. If the nail bends during hammering, a human intervenes and straightens it with a wrench. For comparison, 14 humans (2 females and 12 males) perform the same single-hand hammering task under identical conditions, using the same wooden board, nail, and hammer. For human participants, it takes an average 13.15 strikes with a standard deviation of 6.41 to accomplish the task. On the other hand, ARMADA achieves a comparable level of efficiency to humans, driving the nail with an average of 10 strikes with a standard deviation of 1.26. Please see our supplement video on hammering to better grasp the speed and impact that ARMADA can generate.

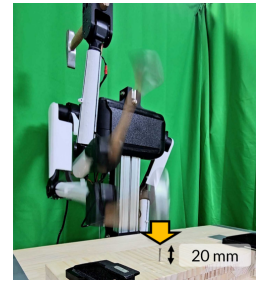


Fig. 10: Hammering experiment setup. A nail is fixed on a wooden board with a height of 20 mm. The robot repeatedly strikes the nail until fully driven into the board.

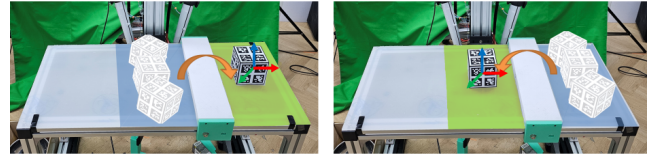


Fig. 11: (a) Scenario 1: The robot moves the object from the right to the left of the bump. (b) Scenario 2: The robot moves the object from the left to the right. The object’s initial pose is randomly set within the blue area. The robot must manipulate the object to match both the position and orientation of the goal pose sampled within the green area.

B. RL-based non-prehensile manipulation

To validate our claim that ARMADA can be used for RL, we train ARMADA on a contact-rich non-prehensile manipulation task entirely in simulation and zero-shot transfer the policy to the real world. In this task, the robot uses a single arm to manipulate a cube whose length is 90mm over a 25 mm bump obstacle on the table, as shown in Figure 11. Starting from a random initial pose, the robot must push, topple, strike, and reorient the object to overcome the bump and put it at the specified goal position and orientation without dropping it. We train the policy using NVIDIA Isaac Gym [43] with extensive domain randomization and zero-shot transfer to the real robot. Details regarding the training including hyperparameters and MDP definitions are in Appendix.

We perform 20 trials in total, 10 on each scenario. ARMADA achieves a 9/10 success rate in scenario 1, with a single failure where the cube falls off the table during the manipulation. In scenario 2, it achieves 7/10, where failures occur because the robot fails to make solid contact with the object. Most of the errors happen because of the sim-to-real gap in the environment and object, such as the object friction coefficient. Overall, the robot demonstrates 80% success rate across both scenarios.

C. Human motion shadowing: Bimanual throwing

In this task, we re-target human joint poses to the robot to show that ARMADA can serve as the platform for learning dynamic motions from a human demonstration. We use

WHAM [52] to predict SMPL [41] parameters, which estimate human joint keypoints, joint angles, and body shape to describe the pose of the human body. However, simply copying the joint angles to the corresponding actuators results in inaccurate motion due to the discrepancy of morphology between the SMPL model and ARMADA. We instead track the positions of the elbow and wrist joints of the human operator and solve differential inverse kinematics using PINK [10] to find the joint configuration that minimizes the distance between the robot and the human joints at the elbow and wrist. This enables ARMADA to mimic human motion while preserving the relative position between the two hands, which is crucial in a bimanual task.

TABLE IV: Box driving distance

Trial	1	2	3	4	5	Avg.	Std dev.
Distance (m)	1.80	2.07	1.81	2.20	2.25	2.03	0.19

To show that ARMADA can shadow dynamic motion, we perform bimanual throwing task where the human shows a quick motion for throwing a box, and the robot’s goal is to mimic that behavior to throw a box (318 g) placed 515 mm above the ground and 300 mm in front of its base as quickly as possible. The overall process of throwing is shown in Figure 1d. Since the driving distance of the box is directly proportional to the end-effector speed at the moment of release, we measure the distance between the base and the closest part of the box. We repeat the experiment 5 times. ARMADA throws the box 2.03 m on average, as shown in Table IV, and during throwing, ARMADA achieves an average maximum speed of 3.56 m/s with the left hand and 3.92 m/s with the right hand. To view the more detailed motion of ARMADA, please see our supplement video on bimanual throwing.

VI. LIMITATION

The use of 3D-printed PLA for structural components improves improving ease of assembly and reduces weight and cost, yet it causes deformation under heavy load, which can diminish end-effector precision. Using metal, such as aluminum, would remedy this problem. Additionally, ARMADA relies on integrated joint relative encoders, requiring manual initialization in a fixed joint configuration each time the system is powered on. Using absolute joint encoders could significantly improve accuracy and ease of use, although it would increase the overall cost.

The 6 DoF configuration of the arm provides sufficient mobility for single-arm manipulation tasks, yet it shows a limitation in certain bimanual manipulation problems. Specifically, when ARMADA holds onto a rigid object with both hands, each arm loses 1 DoF because the hands are fixed to the object during grasping. This leads to an underactuated kinematic chain which has a limited mobility in 3D space. We can achieve more mobility by letting the object slip inside the grippers, yet this renders the grasp less robust and simulation difficult. Therefore, we anticipate that designing a lightweight

3 DoF wrist in place of the current 2 DoF wrist allows a more diverse repertoire of manipulation in bimanual tasks.

Finally, the limited torque density of commercially available proprioceptive actuators restricts the performance. Currently, all of our actuators feature a 1:10 gear ratio, so ARMADA can handle up to 2.5 kg of payload. To handle a heavier object and manipulate it with higher torque, we expect the actuator to have 1:20~30 gear ratio, but it is difficult to find an off-the-shelf product that meets our requirements. Customizing the actuator to increase the torque density while minimizing the weight will enable ARMADA to move faster and handle more diverse objects.

REFERENCES

- [1] Manipulating industrial robots – performance criteria and related test methods. Technical Report ISO 9283:1998, International Organization for Standardization, 1998.
- [2] Jiri Adamec, Peter Hofer, Stefan Pittner, Fabio Monticelli, Matthias Graw, and Jutta Schöpper. Biomechanical assessment of various punching techniques. *International journal of legal medicine*, 135:853–859, 2021.
- [3] Alin Albu-Schäffer, Sami Haddadin, Ch Ott, Andreas Stemmer, Thomas Wimböck, and Gerhard Hirzinger. The dlr lightweight robot: design and control concepts for robots in human environments. *Industrial Robot: an international journal*, 34(5):376–385, 2007.
- [4] Arthur Allshire, Mayank Mittal, Varun Lodaya, Viktor Makoviychuk, Denys Makoviichuk, Felix Widmaier, Manuel Wüthrich, Stefan Bauer, Ankur Handa, and Animesh Garg. Transferring dexterous manipulation from gpu simulation to a remote real-world trifinger. In *2022 IEEE/RSJ International Conference on Intelligent Robots and Systems (IROS)*, pages 11802–11809. IEEE, 2022.
- [5] OpenAI: Marcin Andrychowicz, Bowen Baker, Maciek Chociej, Rafal Jozefowicz, Bob McGrew, Jakub Pachocki, Arthur Petron, Matthias Plappert, Glenn Powell, Alex Ray, et al. Learning dexterous in-hand manipulation. *The International Journal of Robotics Research*, 39(1):3–20, 2020.
- [6] Georg Bätz, Arhan Yaqub, Haiyan Wu, Kolja Kühnlenz, Dirk Wollherr, and Martin Buss. Dynamic manipulation: Nonprehensile ball catching. In *18th Mediterranean Conference on Control and Automation, MED’10*, pages 365–370. IEEE, 2010.
- [7] RC Beecher. Puma: Programmable universal machine for assembly. In *Computer vision and sensor-based robots*, pages 141–152. Springer, 1979.
- [8] Gerardo Bledt, Matthew J Powell, Benjamin Katz, Jared Di Carlo, Patrick M Wensing, and Sangbae Kim. Mit cheetah 3: Design and control of a robust, dynamic quadruped robot. In *2018 IEEE/RSJ International Conference on Intelligent Robots and Systems (IROS)*, pages 2245–2252. IEEE, 2018.
- [9] Michael Bombile and Aude Billard. Dual-arm control for coordinated fast grabbing and tossing of an object:

- Proposing a new approach. *IEEE Robotics & Automation Magazine*, 29(3):127–138, 2022.
- [10] Stéphane Caron, Yann De Mont-Marin, Rohan Budhiraja, Seung Hyeon Bang, Ivan Domrachev, and Simeon Nedelchev. Pink: Python inverse kinematics based on Pinocchio, 2024.
 - [11] Tao Chen, Jie Xu, and Pulkit Agrawal. A system for general in-hand object re-orientation. In *Conference on Robot Learning (CoRL)*, pages 297–307. PMLR, 2022.
 - [12] Xuxin Cheng, Kexin Shi, Ananye Agarwal, and Deepak Pathak. Extreme parkour with legged robots. In *2024 IEEE International Conference on Robotics and Automation (ICRA)*, pages 11443–11450. IEEE, 2024.
 - [13] Yoonyoung Cho, Junhyek Han, Yoontae Cho, and Beomjoon Kim. Corn: Contact-based object representation for nonprehensile manipulation of general unseen objects. 2024.
 - [14] Suyoung Choi, Gwanghyeon Ji, Jeongsoo Park, Hyeonjun Kim, Juhyeok Mun, Jeong Hyun Lee, and Jemin Hwangbo. Learning quadrupedal locomotion on deformable terrain. *Science Robotics*, 8(74):eade2256, 2023.
 - [15] Jr George C Devol. Programmed article transfer, June 13 1961. US Patent 2,988,237.
 - [16] Zipeng Fu, Qingqing Zhao, Qi Wu, Gordon Wetzstein, and Chelsea Finn. Humanplus: Humanoid shadowing and imitation from humans. *Conference on Robot Learning (CoRL)*, 2024.
 - [17] Manolo Garabini, Andrea Passaglia, Felipe Belo, Paolo Salaris, and Antonio Bicchi. Optimality principles in variable stiffness control: The vsa hammer. In *2011 IEEE/RSJ International Conference on Intelligent Robots and Systems*, pages 3770–3775. IEEE, 2011.
 - [18] David V Gealy, Stephen McKinley, Brent Yi, Philipp Wu, Phillip R Downey, Greg Balke, Allan Zhao, Menglong Guo, Rachel Thomasson, Anthony Sinclair, et al. Quasi-direct drive for low-cost compliant robotic manipulation. In *2019 International Conference on Robotics and Automation (ICRA)*, pages 437–443. IEEE, 2019.
 - [19] Ali Ghadirzadeh, Atsuto Maki, Danica Kragic, and Mårten Björkman. Deep predictive policy training using reinforcement learning. In *2017 IEEE/RSJ International Conference on Intelligent Robots and Systems (IROS)*, pages 2351–2358, 2017.
 - [20] Simon Guist, Jan Schneider, Hao Ma, Le Chen, Vincent Berenz, Julian Martus, Heiko Ott, Felix Grüniger, Michael Muehlebach, Jonathan Fiene, et al. Safe & accurate at speed with tendons: A robot arm for exploring dynamic motion. In *RSS 2024 Workshop: Data Generation for Robotics*, 2024.
 - [21] Sami Haddadin, Sven Parusel, Lars Johannsmeier, Saskia Golz, Simon Gabl, Florian Walch, Mohamadreza Sabaghian, Christoph Jähne, Lukas Hausperger, and Simon Haddadin. The franka emika robot: A reference platform for robotics research and education. *IEEE Robotics & Automation Magazine*, 29(2):46–64, 2022.
 - [22] Ankur Handa, Arthur Allshire, Viktor Makoviychuk, Aleksei Petrenko, Ritvik Singh, Jingzhou Liu, Denys Makoviichuk, Karl Van Wyk, Alexander Zhurkevich, Balakumar Sundaralingam, et al. Dextreme: Transfer of agile in-hand manipulation from simulation to reality. In *2023 IEEE International Conference on Robotics and Automation (ICRA)*, pages 5977–5984. IEEE, 2023.
 - [23] Tairan He, Zhengyi Luo, Xialin He, Wenli Xiao, Chong Zhang, Weinan Zhang, Kris Kitani, Changliu Liu, and Guanya Shi. Omnih2o: Universal and dexterous human-to-humanoid whole-body teleoperation and learning. *arXiv preprint arXiv:2406.08858*, 2024.
 - [24] Tairan He, Zhengyi Luo, Wenli Xiao, Chong Zhang, Kris Kitani, Changliu Liu, and Guanya Shi. Learning human-to-humanoid real-time whole-body teleoperation. *2024 IEEE/RSJ International Conference on Intelligent Robots and Systems (IROS)*, 2024.
 - [25] Gerd Hirzinger, A Albu-Schaffer, M Hahnle, Ingo Schaefer, and Norbert Sporer. On a new generation of torque controlled light-weight robots. In *Proceedings 2001 ICRA. IEEE International Conference on Robotics and Automation (Cat. No. 01CH37164)*, volume 4, pages 3356–3363. IEEE, 2001.
 - [26] Gerd Hirzinger, Norbert Sporer, Alin Albu-Schaffer, M Hahnle, Rainer Krenn, Antonio Pascucci, and Markus Schedl. Dlr’s torque-controlled light weight robot iii—are we reaching the technological limits now? In *Proceedings 2002 IEEE International Conference on Robotics and Automation (Cat. No. 02CH37292)*, volume 2, pages 1710–1716. IEEE, 2002.
 - [27] David Hoeller, Nikita Rudin, Dhionis Sako, and Marco Hutter. Anymal parkour: Learning agile navigation for quadrupedal robots. *Science Robotics*, 9(88):eadi7566, 2024.
 - [28] Jwu-Sheng Hu, Ming-Chih Chien, Yung-Jung Chang, Shyh-Haur Su, and Chen-Yu Kai. A ball-throwing robot with visual feedback. In *2010 IEEE/RSJ International Conference on Intelligent Robots and Systems*, pages 2511–2512, 2010.
 - [29] Abid Imran and Byung-Ju Yi. Impulse modeling and analysis of dual arm hammering task: Human-like manipulator. In *2016 IEEE/RSJ International Conference on Intelligent Robots and Systems (IROS)*, pages 362–367. IEEE, 2016.
 - [30] Teruyuki IZUMI and Yoshikazu HITAKA. Control of a hitting velocity and direction for a hammering robot using a flexible link. *Journal of the Robotics Society of Japan*, 11(3):436–443, 1993.
 - [31] Yan-Bin Jia, Matthew Gardner, and Xiaoqian Mu. Batting an in-flight object to the target. *The International Journal of Robotics Research*, 38(4):451–485, 2019.
 - [32] Minchan Kim, Junhyek Han, Jaehyung Kim, and Beomjoon Kim. Pre-and post-contact policy decomposition for non-prehensile manipulation with zero-shot sim-to-real transfer. In *2023 IEEE/RSJ International Conference on Intelligent Robots and Systems (IROS)*,

- pages 10644–10651. IEEE, 2023.
- [33] Seungsu Kim and Aude Billard. Estimating the non-linear dynamics of free-flying objects. *Robotics and Autonomous Systems*, 60(9):1108–1122, 2012.
 - [34] Seungsu Kim, Ashwini Shukla, and Aude Billard. Catching objects in flight. *IEEE Transactions on Robotics*, 30(5):1049–1065, 2014.
 - [35] Yong-Jae Kim. Design of low inertia manipulator with high stiffness and strength using tension amplifying mechanisms. In *2015 IEEE/RSJ International Conference on Intelligent Robots and Systems (IROS)*, pages 5850–5856. IEEE, 2015.
 - [36] Yong-Jae Kim. Anthropomorphic low-inertia high-stiffness manipulator for high-speed safe interaction. *IEEE Transactions on robotics*, 33(6):1358–1374, 2017.
 - [37] Roberto Lampariello, Duy Nguyen-Tuong, Claudio Castellini, Gerd Hirzinger, and Jan Peters. Trajectory planning for optimal robot catching in real-time. In *2011 IEEE International Conference on Robotics and Automation*, pages 3719–3726, 2011.
 - [38] Jiefeng Li, Chao Xu, Zhicun Chen, Siyuan Bian, Lixin Yang, and Cewu Lu. Hybrik: A hybrid analytical-neural inverse kinematics solution for 3d human pose and shape estimation. In *Proceedings of the IEEE/CVF conference on computer vision and pattern recognition*, pages 3383–3393, 2021.
 - [39] Jinhan Li, Yifeng Zhu, Yuqi Xie, Zhenyu Jiang, Mingyo Seo, Georgios Pavlakos, and Yuke Zhu. Okami: Teaching humanoid robots manipulation skills through single video imitation. In *Conference on Robot Learning (CoRL)*, 2024.
 - [40] Guangjun Liu, Xiaojia He, Jing Yuan, Sajan Abdul, and Andrew A Goldenberg. Development of modular and reconfigurable robot with multiple working modes. In *2008 IEEE International Conference on Robotics and Automation*, pages 3502–3507. IEEE, 2008.
 - [41] Matthew Loper, Naureen Mahmood, Javier Romero, Gerard Pons-Moll, and Michael J Black. Smpl: A skinned multi-person linear model. In *Seminal Graphics Papers: Pushing the Boundaries, Volume 2*, pages 851–866. 2023.
 - [42] H Makino and N Furuya. Selective compliance assembly robot arm. In *1st International Conference on Assembly Automation (ICAA)*, pages 77–86, Brighton, mar 1980.
 - [43] Viktor Makoviychuk, Lukasz Wawrzyniak, Yunrong Guo, Michelle Lu, Kier Storey, Miles Macklin, David Hoeller, Nikita Rudin, Arthur Allshire, Ankur Handa, et al. Isaac gym: High performance gpu-based physics simulation for robot learning. *arXiv preprint arXiv:2108.10470*, 2021.
 - [44] Kazutoshi Nishii, Akira Hatano, and Yoshihiro Okumatsu. Ultra-low inertia 6-dof manipulator arm for touching the world. In *2023 IEEE/RSJ International Conference on Intelligent Robots and Systems (IROS)*, pages 432–438. IEEE, 2023.
 - [45] Georgios Pavlakos, Dandan Shan, Ilija Radosavovic, Angjoo Kanazawa, David F. Fouhey, and Jitendra Malik. Reconstructing hands in 3d with transformers. *2024 IEEE/CVF Conference on Computer Vision and Pattern Recognition (CVPR)*, 2023.
 - [46] Morgan Quigley, Alan Asbeck, and Andrew Ng. A low-cost compliant 7-dof robotic manipulator. In *2011 IEEE International Conference on Robotics and Automation*, pages 6051–6058. IEEE, 2011.
 - [47] Vladyslav Romanyuk, Sina Soleymannpour, and Guangjun Liu. A multiple working mode approach to hammering with a modular reconfigurable robot. In *2019 IEEE International Conference on Mechatronics and Automation (ICMA)*, pages 774–779. IEEE, 2019.
 - [48] Brian Rooks. The harmonious robot. *Industrial Robot: An International Journal*, 33(2):125–130, 2006.
 - [49] Seyed Sina Mirrazavi Salehian, Mahdi Khoramshahi, and Aude Billard. A dynamical system approach for softly catching a flying object: Theory and experiment. *IEEE Transactions on Robotics*, 32(2):462–471, 2016.
 - [50] Taku Senoo, Akio Namiki, and Masatoshi Ishikawa. Ball control in high-speed batting motion using hybrid trajectory generator. In *Proceedings 2006 IEEE International Conference on Robotics and Automation, 2006. ICRA 2006.*, pages 1762–1767. IEEE, 2006.
 - [51] Taku Senoo, Akio Namiki, and Masatoshi Ishikawa. High-speed throwing motion based on kinetic chain approach. In *2008 IEEE/RSJ International Conference on Intelligent Robots and Systems*, pages 3206–3211, 2008. doi: 10.1109/IROS.2008.4651142.
 - [52] Soyong Shin, Juyong Kim, Eni Halilaj, and Michael J. Black. Wham: Reconstructing world-grounded humans with accurate 3d motion. *2024 IEEE/CVF Conference on Computer Vision and Pattern Recognition (CVPR)*, 2023.
 - [53] Young-Ha Shin, Seungwoo Hong, Sangyoung Woo, JongHun Choe, Harim Son, Gijeong Kim, Joon-Ha Kim, KangKyu Lee, Jemin Hwangbo, and Hae-Won Park. Design of kaist hound, a quadruped robot platform for fast and efficient locomotion with mixed-integer nonlinear optimization of a gear train. In *2022 International Conference on Robotics and Automation (ICRA)*, pages 6614–6620. IEEE, 2022.
 - [54] Hansol Song, Yun-Soo Kim, Junsuk Yoon, Seong-Ho Yun, Jiwon Seo, and Yong-Jae Kim. Development of low-inertia high-stiffness manipulator limbs2 for high-speed manipulation of foldable objects. In *2018 IEEE/RSJ International Conference on Intelligent Robots and Systems (IROS)*, pages 4145–4151. IEEE, 2018.
 - [55] Timothy J Walilko, David C Viano, and Cynthia A Bir. Biomechanics of the head for olympic boxer punches to the face. *British journal of sports medicine*, 39(10):710–719, 2005.
 - [56] Patrick M Wensing, Albert Wang, Sangok Seok, David Otten, Jeffrey Lang, and Sangbae Kim. Proprioceptive actuator design in the mit cheetah: Impact mitigation and high-bandwidth physical interaction for dynamic legged robots. *Ieee transactions on robotics*, 33(3):509–522, 2017.

- [57] Lei Yan, Theodoros Stouraitis, João Moura, Wenfu Xu, Michael Gienger, and Sethu Vijayakumar. Impact-aware bimanual catching of large-momentum objects. *IEEE Transactions on Robotics*, 2024.
- [58] Vickie Ye, Georgios Pavlakos, Jitendra Malik, and Angjoo Kanazawa. Decoupling human and camera motion from videos in the wild. In *Proceedings of the IEEE/CVF conference on computer vision and pattern recognition*, 2023.
- [59] Andy Zeng, Shuran Song, Johnny Lee, Alberto Rodriguez, and Thomas Funkhouser. Tossingbot: Learning to throw arbitrary objects with residual physics. *IEEE Transactions on Robotics*, 36(4):1307–1319, 2020.
- [60] Wenxuan Zhou and David Held. Learning to grasp the ungraspable with emergent extrinsic dexterity. In *Conference on Robot Learning (CoRL)*, pages 150–160. PMLR, 2023.
- [61] Wenxuan Zhou, Bowen Jiang, Fan Yang, Chris Paxton, and David Held. Hacman: Learning hybrid actor-critic maps for 6d non-prehensile manipulation. 2023.
- [62] Taoyuanmin Zhu. *Design of a Highly Dynamic Humanoid Robot*. Phd thesis, University of California, Los Angeles, 2023.
- [63] Ziwen Zhuang, Zipeng Fu, Jianren Wang, Christopher Atkeson, Sören Schwertfeger, Chelsea Finn, and Hang Zhao. Robot parkour learning. In *Conference on Robot Learning (CoRL)*, 2023.